

Pathways for Conformational Interconversion of Calix[4]arenes

Stefan Fischer,[†] Peter D. J. Grootenhuys,[§] Leo C. Groenen,[‡] Willem P. van Hoorn,[‡] Frank C. J. M. van Veggel,[‡] David N. Reinhoudt,[‡] and Martin Karplus^{*,†}

Contribution from the Department of Chemistry, Harvard University, 12 Oxford Street, Cambridge, Massachusetts 02138, Laboratory of Organic Chemistry, University of Twente, P.O. Box 217, 7500 AE Enschede, The Netherlands, and N.V. Organon International, P.O. Box 20, 5340 BH Oss, The Netherlands

Received June 27, 1994[Ⓢ]

Abstract: Conformational optimization and reaction path calculations are performed on [1,4]metacyclophane **3a** and calix[4]arenes **1a** and **2b** using the CHARMM force field. For each of these compounds, a comprehensive search for all stable conformers was followed by an exhaustive exploration of the several hundred possible pathways between these conformers. The method employed for finding the reaction paths, Conjugate Peak Refinement, proved to be robust and reliable, allowing the connectivity of the complex potential energy surfaces to be charted. The relative stability of the four characteristic conformers agrees with experimental NMR data, except for the Cone form of **2b**. The pathways for Cone inversion in [1,4]metacyclophane **3a** show no preference for a pathway via the 1,2Alt or the 1,3Alt conformers. The conformational entropy corrected energy barriers $\Delta E_{\text{conf}}^{\ddagger}$ are 3.1 and 3.3 kcal/mol, respectively. For **1a**, a stepwise pathway via the 1,2Alt conformer is found to be preferred for the Cone \rightarrow inverted-Cone conversion. The rate-limiting step is the transition from Cone to Paco, with a barrier of activation $\Delta E_{\text{conf}}^{\ddagger} = 14.5$ kcal/mol, comparable to the experimental $\Delta H^{\ddagger} = 14.2$ kcal/mol. Conversion from the key Paco intermediate to the other characteristic conformers was investigated in detail in **2b**. The $\Delta E_{\text{pot}}^{\ddagger}$ values for the conversion from the most stable Paco to Cone, 1,2Alt, and 1,3Alt conformers are 19.6, 20.2, and 18.2 kcal/mol respectively, in qualitative agreement with the relative rates deduced from 2D EXSY NMR. Paths for the transition from inward to outward orientation of the methoxy moieties of **2b** are calculated. The corresponding activation barriers for the rotation of a methoxy group are in the 6–8 kcal/mol range, consistent with the upper bound obtained from the NMR time scale.

Introduction

Calix[4]arenes are macrocyclic compounds which consist of four phenol rings connected via methylene bridges located ortho to the hydroxyl groups. The rings cannot be coplanar and they adopt an orientation that makes the molecule appear like a cup or a chalice. They are being used increasingly in supramolecular chemistry as building blocks for larger molecules that are designed for the complexation of cations or neutral molecules.¹ One interesting property of calix[4]arenes is that they have four characteristic nonplanar conformations, designated as the Cone, the partial Cone (Paco), the 1,2-alternate (1,2Alt), and the 1,3-alternate (1,3Alt) (see Figure 1). Several studies have been published in which the relative stability of the calix[4]arene conformations has been calculated with molecular mechanics,^{2–4} but the relative stability of the four conformations of calix[4]arenes **2** in CDCl₃ found by NMR^{4a,5–7} was not reproduced

exactly. Grootenhuys *et al.*² used MACROMODEL⁸ (AMBER and MM2 force fields), MM2P,⁹ AMBER,¹⁰ and QUANTA/CHARMM¹¹ to calculate the relative stability of the four conformations of **2c**. The force fields showed pronounced differences, which were mainly caused by differences in the electrostatic energy. Only MM2P and QUANTA/CHARMM calculated the partial cone to have the lowest energy, in accord with the NMR data. Using the MM3¹² force field, Shinkai *et al.*⁴ obtained good agreement for the relative stability of the four conformers of **2a** and **2b** between the NMR data and the calculated energies, including vibrational contributions estimated from normal modes.

Measurements with NMR spectroscopy have shown that calix[4]arenes with hydroxyl moieties at the lower rim (**1**) adopt the Cone conformation in CDCl₃ solution,¹³ which is also the structure found in crystals.¹⁴ The stability of the Cone conformation is believed to be caused by a circular array of

[†] Harvard University.[‡] University of Twente.[§] N.V. Organon International.[Ⓢ] Abstract published in *Advance ACS Abstracts*, December 1, 1994.

(1) (a) Gutsche, C. D. *Calixarenes*; Royal Society of Chemistry: Cambridge, 1989. (b) *Calixarenes. A versatile Class of Compounds*; Vicens, J., Böhrner, V., Eds.; Kluwer Academic Publishers: Dordrecht, The Netherlands, 1991. (c) Groenen, L. C.; Reinhoudt, D. N. *Supramolecular Chemistry*; Balzani, V., de Cola, L., Eds.; Kluwer Academic Publishers: Dordrecht, The Netherlands, 1991; pp 51–70.

(2) Grootenhuys, P. D. J.; Kollman, P. A.; Groenen, L. C.; Reinhoudt, D. N.; van Hummel, G. J.; Ugozzoli, F.; Andreotti, G. D. *J. Am. Chem. Soc.* **1990**, *112*, 4165–4176.

(3) Royer, J.; Bayard, F.; Decoret, C. *J. Chim. Phys.* **1990**, *87*, 1695–1700.

(4) (a) Harada, T.; Rudziński, J. M.; Shinkai, S. *J. Chem. Soc., Perkin Trans. 2* **1992**, 2109–2115. (b) Harada, T.; Rudziński, J. M.; Osawa, E.; Shinkai, S. *Tetrahedron* **1993**, *49*, 5941–5954.

(5) Iwamoto, K.; Araki, K.; Shinkai, S. *J. Org. Chem.* **1991**, *56*, 4955–4962.

(6) Gutsche, C. D.; Dhawan, B.; Levine, J. A.; No, K. H.; Bauer, L. J. *Tetrahedron* **1983**, *39*, 409–426.

(7) Groenen, L. C.; van Loon, J.-D.; Verboom, W.; Harkema, S.; Casnati, A.; Ungaro, R.; Pochini, A.; Ugozzoli, F.; Reinhoudt, D. N. *J. Am. Chem. Soc.* **1991**, *113*, 2385–2392.

(8) MACROMODEL Version 1.5: Still, W. C.; Department of Chemistry, Columbia University, New York, 1987.

(9) MM2P(85): Sprague, J. T.; Tai, J. C.; Yuh, Y.; Allinger, N. L. *J. Comput. Chem.* **1987**, *8*, 581–603.

(10) AMBER 3.0: Singh, U. C.; Weiner, P. K.; Caldwell, J.; Kollman, P. A. University of California—San Francisco, 1987.

(11) QUANTA 2.1A: Polygen Corp., Waltham, MA.

(12) (a) Allinger, N. L.; Yuh, Y. H.; Lii, J.-H. *J. Am. Chem. Soc.* **1989**, *111*, 8551–8566. (b) Lii, J.-H.; Allinger, N. L. *J. Am. Chem. Soc.* **1989**, *111*, 8566–8575. (c) Lii, J.-H.; Allinger, N. L. *J. Am. Chem. Soc.* **1989**, *111*, 8576–8582.

(13) (a) Happel, G.; Mathiasch, B.; Kämmerer, H. *Macromol. Chem.* **1975**, *176*, 3317–3334. (b) Gutsche, C. D.; Bauer, J. *J. Am. Chem. Soc.* **1985**, *107*, 6052–6059. (c) Araki, K.; Shinkai, S.; Matsuda, T. *Chem. Lett.* **1989**, 581–584.

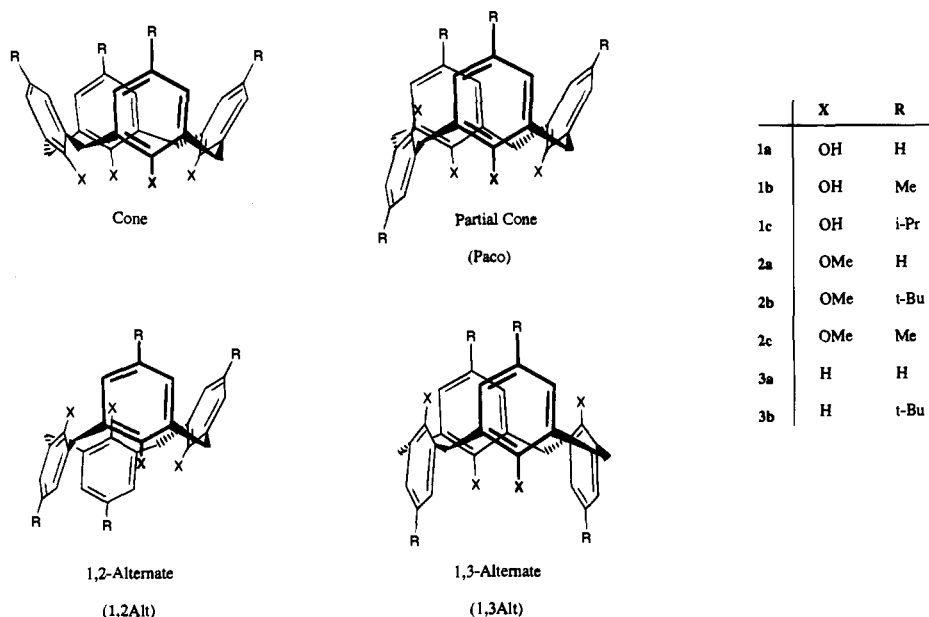


Figure 1. The four characteristic conformers of [14]metacyclophanes and calix[4]arenes.

very strong hydrogen bonds, in which the OH groups at the lower rim act as both donors and acceptors. The calix[4]arenes **1** are still conformationally flexible, because the two equivalent Cone conformations (with the four oxygen atoms either all up or all down) can interconvert. Several mechanisms for interconversion have been proposed. One is a "broken-chain" mechanism, in which the array of H-bonds is broken and the 1,3Alt form is the intermediate;^{13a} another is a "continuous-chain" mechanism, in which the hydrogen bonds remain mostly intact and a skewed 1,2Alt-like intermediate is involved.^{13b} Some authors have suggested that the interconversion of tetrahydrocalix[4]arenes is a concerted process in which more than one phenol ring rotate simultaneously.^{13a,c,15} In all proposed mechanisms the hydroxyl moieties swing through the annulus, since the upper rim (bearing the R groups in Figure 1) is too large to pass through the annulus.

The calix[4]arene derivatives **2** exist in CDCl₃ solution at room temperature as a mixture of all four characteristic conformations, as determined by ¹H and 2D NMR measurements.^{4a,5-7} In decreasing order, the relative stability of **2b** is Paco (most stable) > 1,2Alt > Cone > 1,3Alt. The conformers interconvert rapidly, with the Paco conformer as the key intermediate, as indicated by 2D EXSY NMR spectra showing cross-peaks for Paco/Cone and Paco/1,3Alt conformations.^{7,16} Each of the other three conformations can be formed from the Paco conformation by the rotation of only one anisole ring. The methoxy moiety passes through the annulus during the ring-flips. Conformational interconversion is no longer possible at room temperature when the methoxy moieties in **2b** are replaced by ethoxy groups. Solvent effects in CDCl₃ play a minor role, although compounds **2b** and **3b** are capable of complexing solvent molecules in the cavity formed by the four *p*-*tert*-butyl groups in the Cone form, as seen in the X-ray crystal structures of complexes with toluene,¹⁴ MeCN,¹⁷ or *p*-phenylcalix[4]arene complexed with CHCl₃.¹⁸

The [14]metacyclophanes **3** have recently been synthesized.^{19,20} These compounds are more flexible than either **1** or **2**. No single characteristic conformation could be shown to be

the most stable by NMR in CDCl₂F solution. Because [14]-metacyclophanes have the same skeleton as the calix[4]arenes, investigation of [14]metacyclophanes can yield insight into the influence of the lower rim substitute (X in Figure 1) and the skeleton on the properties of calix[4]arenes.^{4b,21}

Recently, an algorithm has been developed for finding reaction pathways and transition states involving many degrees of freedom.²² This algorithm, called Conjugate Peak Refinement (CPR), yields a series of true saddle points which are connected to one another through minimum energy paths composed of a string of structures. The resulting path forms a continuous reaction coordinate between a given reactant and a given product. Unlike a trajectory obtained from molecular dynamics, which includes many fluctuations uncorrelated to the progress of the reaction, the reaction trajectory involves only the minimal amount of necessary motions. In the low-temperature limit, this sequence of conformations is the most probable path. At normal temperatures, it is likely to be a good approximation to the path obtained by averaging over the dynamic pathways, particularly if the conformational change is dominated by the energy rather than by entropy. CPR is currently the only available method for finding adiabatic reaction paths that is fully automated and reliable for systems that have complex energy surfaces involving a very large number of degrees of freedom. The CPR algorithm is integrated in the CHARMM²³ program and has been successfully applied to the tyrosine ring-flip in BPTI,²⁴ to the closure of the lid over the catalytic site of triosephosphate isomerase,²⁵ and to the mechanism of rotamase catalysis by FKBP.²⁶ Here, we use the CPR algorithm to exhaustively explore the conformational intercon-

(17) McKervey, M. A.; Seward, E. M.; Ferguson, G.; Ruhl, B. L. *J. Org. Chem.* **1986**, *51*, 3581-3584.

(18) Juneja, R. K.; Robinson, K. D.; Johnson, C. P.; Atwood, J. L. *J. Am. Chem. Soc.* **1993**, *115*, 3818-3819.

(19) (a) Ting, Y.; Verboom, W.; Groenen, L. C.; van Loon, J.-D.; Reinhoudt, D. N. *J. Chem. Soc., Chem. Commun.* **1990**, 1432-1433. (b) Goren, Z.; Biali, S. E. *J. Chem. Soc., Perkin Trans. 1* **1990**, 1484-1487. (c) Grynszpan, F.; Goren, Z.; Biali, S. E. *J. Org. Chem.* **1991**, *56*, 532-536. (d) Grynszpan, F.; Biali, S. F. *Tetrahedron Lett.* **1991**, *32*, 5155-5158.

(20) McMurry, J. E.; Phelan, J. C. *Tetrahedron Lett.* **1991**, *32*, 5655-5658.

(21) Jaime, C.; de Mendoza, J.; Prados, P.; Nieto, P. M.; Sánchez, C. *J. Org. Chem.* **1991**, *56*, 3372-3376.

(22) Fischer, S.; Karplus, M. *Chem. Phys. Lett.* **1992**, *194*, 252-261.

(23) Brooks, B. R.; Bruccoleri, R. E.; Olafson, B. D.; States, D. J.; Swaminathan, S.; Karplus, M. *J. Comp. Chem.* **1983**, *4*, 187-217.

(14) Andreotti, G. D.; Ungaro, R.; Pochini, A. *J. Chem. Soc., Chem. Commun.* **1979**, 1005-1007.

(15) Groenen, L. C.; Steinwender, E.; Lutz, B. T. G.; van der Maas, J. H.; Reinhoudt, D. N. *J. Chem. Soc., Perkin Trans. 2* **1992**, 1893-1898.

(16) van Loon, J.-D.; Groenen, L. C.; Verboom, W.; Wijmenga, S. S.; Reinhoudt, D. N. *J. Am. Chem. Soc.* **1991**, *113*, 2378-2384.

version in [1₄]metacyclophane **3a** and in calix[4]arenes **1a** and **2b**. These compounds are representative of most compounds **1**, **2**, and **3**, because the nature of the upper rim substitutes has only a marginal effect on the total energy of the conformation.² We propose detailed stepwise sequences for interconversion in [1₄]metacyclophanes **3** and in calix[4]arenes **1** and **2**. The corresponding activation barriers of the conformational interconversion in calix[4]arene **1a** enable us to distinguish between the reaction mechanisms proposed for interconversions in **1**.^{13,15} The energies of the transition states in **2b** are compared with kinetic data from ¹H and 2D NMR. Results in agreement with experiment are obtained. They provide new insights into the nature of the transitions and indicate that version 22 of the all-hydrogen CHARMM parameter set²⁷ is appropriate for calix[4]arenes.

Methods

Energy Minimizations. For compounds **1a** and **3a**, the four characteristic conformations were considered and minimized. For compounds **2b**, a systematic search with concomitant energy minimization of all possible in/out orientations of the methoxy groups in each of the four characteristic conformations was performed. The energies of the conformations were minimized by the Conjugate Gradient method and followed by the Newton–Raphson method until the root-mean-square (rms) value of the energy gradient was less than 0.0001 kcal mol⁻¹ Å⁻¹. For compound **1a**, the influence of cooperative polarization of the hydroxyl groups was investigated by varying the charge separation across the O–H bond. The bonded parameters, point charges, and van der Waals parameters were derived from a developmental version of the CHARMM parameters for the tyrosine and aliphatic amino acids side chains and for methyl acetate (see Appendix). A dielectric constant $\epsilon = 1$ was used with no cut-off for the nonbonded interactions. This seems appropriate, since most studies are carried out in weakly polar solvents. All calculations were done with the CHARMM program.²³

Reaction Path Calculations. The Conjugate Peak Refinement (CPR) algorithm²² searches for maxima along the adiabatic energy valley connecting two local minima on an energy surface. These maxima are refined to saddle points and represent the transition states of the reaction pathway between the two minima. The algorithm has been integrated to the CHARMM program²³ in the TRAVEL module. The output of CPR consists of a series of N intermediate structures (each given by its coordinate vector \mathbf{r}_i) along the reaction pathway from the reactant \mathbf{r}_0 to the product \mathbf{r}_{N+1} , including one or more saddle points. The one-dimensional reaction coordinate along this curvilinear path is given by

$$\lambda_i = \sum_{j=0}^{i-1} |\mathbf{r}_{j+1} - \mathbf{r}_j|$$

The path-scanning step size $\Delta\lambda$ (the only parameter of the CPR method which has a system-dependent optimal value) was set initially to 1/6 of the rms difference between reactant and product coordinates. This step size is automatically reduced in TRAVEL until an optimum value is reached.²⁴ The final value of $\Delta\lambda$ was 0.05 Å, except for the calculations on the polarized O–H bonds, where it got reduced to 0.01 Å. Presetting the optimum step size can save some computational overhead. The rms gradients of the saddle points were in the 10⁻⁶–10⁻⁵ kcal mol⁻¹ Å⁻¹ range. In the absence of an initial guess for transition intermediates, the CPR method as implemented in TRAVEL generates a first guess for the pathway by linear interpolation between

(24) Fischer, S. Curvilinear reaction coordinates of conformational change in macromolecules. Application to rotamase catalysis. Ph.D. Thesis, Harvard University, 1992.

(25) Joseph, D.; Fischer, S.; Karplus, M. In preparation.

(26) Fischer, S.; Michnick, S.; Karplus, M. *Biochemistry* **1993**, *32*, 13830–13837.

(27) (a) Smith, J. C.; Karplus, M. *J. Am. Chem. Soc.* **1992**, *114*, 801–812. (b) Dunbrack, R. L., Jr.; Joseph, D.; Karplus, M. To be submitted for publication. (c) MacKerell, A.; Karplus, M.; et al. To be submitted for publication.

the Cartesian coordinates of the reactant and the product. In a few cases, such an initial guess results in a path with some unlikely segments, for example in which a hydrogen passes through the aromatic ring. This problem is easily resolved by continuing the refinement after having excised the undesired segments from the path. After all the saddle points were fully refined by CPR, and for those paths shown here in the figures, the other path points were further relaxed into the adiabatic valleys of the energy by Synchronous Chain Minimization (SCM),²⁸ a path optimization method related to the procedure by Choi and Elber,²⁹ but better behaved in systems with many degrees of freedom.

The pathways for compounds **1a** and **3a** were generated by calculating the following transitions: Cone → Paco, Paco → 1,2Alt, Paco → 1,3Alt, Cone → 1,2Alt, Cone → 1,3Alt, and Cone → inverted Cone (Cone'), all without initial intermediates. Concerted Cone → Cone' pathways in **1a** were obtained by increasing the charge separation on the OH moiety. The Paco is the key intermediate for compound **2b**, therefore the following transitions were calculated for this compound: all Paco conformations to all Cone, 1,2Alt, and 1,3Alt conformations (conformations are described in Table 2). After the lowest-energy interconversion path was found from one characteristic conformation to the other, methyl rotation paths were calculated for each characteristic conformation, in order to find the complete lowest energy path from the ground state of each characteristic conformer to the ground state of every other characteristic conformer. Unless otherwise specified, the transition state energies given here are relative to the energy of the most stable conformer (global energy minimum) of **1a**, **2b**, or **3a**, respectively.

Hammond Postulate. According to Hammond,³⁰ "If two states, as for example, a transition state and an unstable intermediate, occur consecutively during a reaction process and have nearly the same energy content, their interconversion will involve only a small reorganization of the molecular structures". Although the Hammond postulate was formulated for chemical reactions, it is likely to apply also to conformational transitions. Thus, the change in geometry during a conformational interconversion should correlate with the change in energy. The applicability of the postulate was tested by comparing the progress along the reaction coordinate λ (taken relative to a given saddle point) to the change in the energy. For the structures k along the path on each side ($k > 0$ or $k < 0$) of the saddle point ($k = 0$), we define:

$$h_k = |\lambda_k - \lambda_{\text{saddle}}|$$

$$H_k = \text{MAX}(h_k) - h_k$$

To allow a direct comparison of the energy and H_k , the values H_k are scaled so that the amplitude of the change in H_k equals the energy barrier. H_k is plotted as a function of λ_k to show the correlation between changes in the energy and changes in the rms displacement of the atomic coordinates.

Results

(a) Geometry Optimizations. The minimized energies of the four characteristic conformers of compound **3a** are listed in Table 1. These results are very similar to those previously obtained with the MM3 force field.^{4b} Calculations with the MMX force field²⁰ and MM2 force field²¹ also resulted in Cone as the lowest energy conformation. The energy differences between conformers is small, with a maximum value of 1.9 kcal/mol between the Cone and 1,3Alt conformers.

Also listed in Table 1 are the optimized energies of compound **1a**, which are obtained when the four hydroxyls remain in the same orientation relative to their ring. It is the orientation that allows the formation of a circular array of four H-bonds in the Cone. The Cone is the lowest energy conformer, in accordance with ¹H NMR data in various solvents.¹³ Earlier molecular mechanics calculations^{2,3,4b} have yielded the same energy order: Cone < Paco < 1,2Alt < 1,3Alt. Recent calculations

(28) Fischer, S.; Karplus, M. In preparation.

(29) Choi, C.; Elber, R. *J. Chem. Phys.* **1991**, *94*, 751–760.

(30) Hammond, G. S. *J. Am. Chem. Soc.* **1955**, *77*, 334–338.

Table 1. Energy^f (kcal/mol) for the Characteristic Conformers of [1₄]Cyclophane **3a** and of Calix[4]arene **1a**

conf	MM3 ^a	E_{coval}^b	E_{vdW}	E_{elec}	E_{pot}^c	n^d	E_{conf}^f
3a							
Cone	0.0	0.0	0.0	0.0	0.0	2	0.0
Paco	1.2	0.8	1.9	-1.5	1.2	8	0.5
1,2Alt	1.8	1.3	2.3	-1.8	1.8	4	1.5
1,3Alt	1.7	1.1	2.1	-1.3	1.9	2	1.9
1a							
Cone	0.0	0.0	0.0	0.0	0.0	2	0.0
Paco	9.9	1.0	-1.8	10.4	9.6	8	8.9
1,2Alt	11.7	2.9	-2.1	11.0	11.8	4	11.5
1,3Alt	18.7	0.5	-3.5	20.2	17.2	2	17.2

^a Potential energy from ref 4b. ^b $E_{\text{coval}} = E_{\text{bond}} + E_{\text{angle}} + E_{\text{urey}} + E_{\text{dih}} + E_{\text{pot}} + E_{\text{vdW}} + E_{\text{elec}}$. ^c n is the conformational degeneracy of each conformer. ^d $E_{\text{conf}} = E_{\text{pot}} - kT \ln(n)$, at -30 °C. ^e Energies are given relative to the minimum energy Cone form of the respective compound. Absolute energies, particularly the covalent terms, have little significance when empirical energy functions are used.

with the MM3 force field^{4b} yielded very similar energy values (see Table 1). Four H-bonds are present in the Cone conformation, two in the Paco or the 1,2Alt, and none in the 1,3Alt. From Table 1, it can be seen that the relative stability of the conformations of **1a** is essentially determined by the number of hydrogen bonds that can be formed. Each H-bond contributes to lower the electrostatic energy by about 5 kcal/mol. Other molecular mechanics force fields vary in their ability to distinguish between the 1,2Alt (2 hydrogen bonds) and the 1,3Alt (0 hydrogen bonds) conformers: the energy difference is 7.0 kcal/mol for MM3,^{4b} but only 0.1 kcal/mol for MM2P³ and 1.3 kcal/mol for AMBER 3.0.²

The Cone, Paco, and 1,3Alt conformers of **1a** are almost identical to the Cone, Paco, and 1,3Alt conformers of **3a**. The rms differences in the positions of the C-atoms are only 0.1, 0.1, and 0.2 Å, respectively. The 1,2Alt of **3a** differs from the 1,2Alt of **1a** (rms difference 0.8 Å) by the fact that one benzyl ring is rotated away from the annulus. The small differences between the conformations of **1a** and **3a** indicate that near-optimal H-bonds can be formed in **1a** without inducing extra strain in the skeleton of the [1₄]metacyclophane moiety.

Each of the four methoxy groups of the tetramethyl ether compound **2b** can point either toward the center of the annulus (in) or toward the outside (out). For each of the four characteristic conformers of **2b**, a systematic search of all possible in/out orientations of the methoxy groups was performed. It was found that 28 out of the 31 possible conformations are stable. The corresponding local energy minima are listed in Table 2. The most stable conformer is Paco with one methoxy pointing inward. The variation in the potential energy for the various conformers is quite large, up to 27.7 kcal/mol above the Paco ground state. The highest energy conformers are found for the Cone and the Paco states when a majority of the methoxy groups point inward toward each other, resulting in structural distortions as indicated by the large contribution of E_{coval} to the potential energy of these states. The 1,2Alt and the 1,3Alt states can better accommodate the inward pointing methoxy groups, since these are distributed on both sides of the annulus.

(b) Interconversion pathways. **(i) Ring-Flips in [1₄]Metacyclophane 3a.** The transition-state energies for the three saddle points connecting the Paco form to the Cone, 1,2Alt, and 1,3Alt conformers are listed in Table 3. The energy profiles of the corresponding reaction paths are shown in Figure 2. From the connectivity chart in Figure 3A, it is apparent that the Cone → inverted Cone (Cone') conversion with the lowest energy barrier is via the 1,2Alt intermediate, with the rate-limiting step (in terms of energy barriers) being the Cone → Paco transformation, which has an activation barrier of $\Delta E_{\text{pot}}^{\ddagger} = 3.8$ kcal/mol. The energy barrier arises mainly from angle distortion

Table 2. Energy (kcal/mol) of the Conformers of Calix[4]arene **2b**

conf ^a	E_{coval}	E_{vdW}	E_{elec}	E_{pot}	n	E_{conf}
Paco						
0001~ABAA	0.0	0.0	0.0	0.0	8	0.0
0001~AAAA	-7.8	-0.1	9.0	1.1	8	1.1
0001~AAAB	-5.4	0.5	6.1	1.2	8	1.2
0001~ABAB	2.6	1.2	-1.7	2.1	8	2.1
0001~BAAA	-3.6	0.0	5.8	2.2	16	1.9
0001~AABA	1.0	1.5	-0.3	2.2	16	1.9
0001~BABA	2.0	0.2	1.7	3.9	8	3.9
0001~BBAA	8.7	1.6	-1.9	8.4	16	8.1
0001~BABB	10.2	2.1	-3.8	8.5	8	8.5
0001~BBBB	15.8	3.6	-4.7	14.7	16	14.4
0001~BBBB	28.9	3.6	-4.8	27.7	8	27.7
0001~BBBA					8	unstable
1,2Alt						
0011~ABAB	-0.2	1.6	-0.7	0.7	8	0.7
0011~AAAB	-2.1	1.0	2.5	1.4	16	1.1
0011~ABBA	2.5	1.7	-2.0	2.2	8	2.2
0011~AAAA	-4.2	1.7	9.3	6.8	4	7.1
0011~BBBA	7.3	4.4	-2.0	9.7	16	9.4
0011~AABB	4.8	3.5	1.7	10.0	8	10.0
0011~BBBB					4	unstable
1,3Alt						
0101~AAAA	-7.8	-2.0	10.3	0.5	2	1.2
0101~AABA	-5.4	-0.1	6.3	0.8	8	0.8
0101~AABB	-0.9	1.8	0.4	1.3	8	1.3
0101~BABA	-1.7	-0.1	3.8	2.0	4	2.3
0101~ABBB	5.0	3.0	-1.2	6.8	8	6.8
0101~BBBB	12.7	3.5	-2.8	13.4	2	14.1
Cone						
0000~AAAA	-8.4	0.2	12.0	3.8	2	4.5
0000~AABA	2.1	2.0	1.0	5.1	8	5.1
0000~ABAB	6.1	1.9	-0.6	7.4	4	7.7
0000~AABB	12.8	4.9	-2.6	15.1	8	15.1
0000~ABBB	22.1	4.2	-2.8	23.5	8	23.5
0000~BBBB					2	unstable

^a The digits in the names of conformations indicate which anisole ring is inverted. The letters indicate whether the methoxy group attached to each aromatic ring points outwards (A) or inwards (B). For example: 0001~AAAB is a Paco in which the methoxy group on the inverted aromatic ring points inwards. See also caption of Table 1.

Table 3. Energy^a (kcal/mol) of the Transition State in Aromatic Ring-Flipping Reactions

reaction	$E_{\text{coval}}^{\ddagger}$	$E_{\text{vdW}}^{\ddagger}$	$E_{\text{elec}}^{\ddagger}$	$E_{\text{pot}}^{\ddagger}$	n^{\ddagger}	$E_{\text{conf}}^{\ddagger}$
3a						
Cone → Paco	3.0	2.9	-2.1	3.8	8	3.1
Paco → 1,2Alt	2.0	2.4	-1.8	2.6	16	1.6
Paco → 1,3Alt	3.0	3.0	-2.0	4.0	8	3.3
1a						
Cone → Paco	6.5	-0.4	9.1	15.2	8	14.5
Paco → 1,2Alt	4.7	0.9	9.1	14.7	16	13.7
Paco → 1,3Alt	6.2	-1.6	18.2	22.8	8	22.1

^a Energies are relative to the Cone ground state of the respective compound (see also caption of Table 1).

(2.4 kcal/mol) and unfavorable van der Waals interactions (2.8 kcal/mol), which are compensated somewhat by favorable electrostatic interactions (-2.1 kcal/mol). The Cone → Cone' route via the 1,3Alt conformer is only slightly higher in energy; the rate-limiting steps are the Paco → 1,3Alt → Paco' legs, whose transition-state energy relative to the Cone ground state is $E_{\text{pot}}^{\ddagger} = 4.0$ kcal/mol. To search for a concerted reaction (i.e. without the Paco intermediate), a direct refinement of the Cone → Cone' conversion was done with the Cone conformer taken as reactant and the Cone' conformer as product. The resulting pathway was found not to be concerted, but to proceed via the Paco and 1,2Alt intermediates.

Because there are four ways for a Cone conformer to convert into a Paco conformer (by flipping any one of the four benzyl rings), each with a potential energy barrier of $\Delta E_{\text{pot}}^{\ddagger} = 3.8$ kcal/

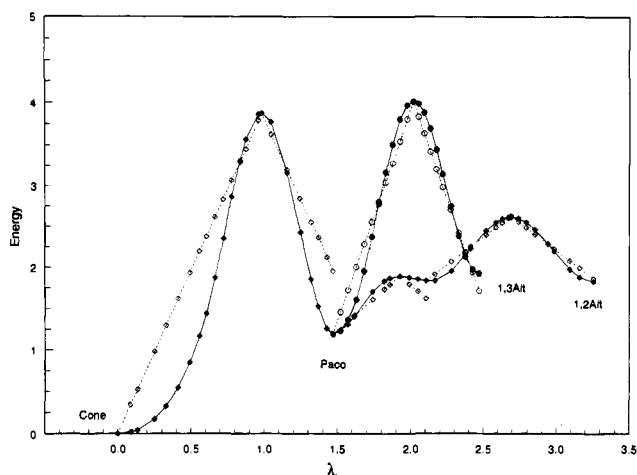


Figure 2. Energy profile (solid line, kcal/mol) and Hammond correlation (dashed line) for the ring-flipping isomerization reactions in compound **3a**.

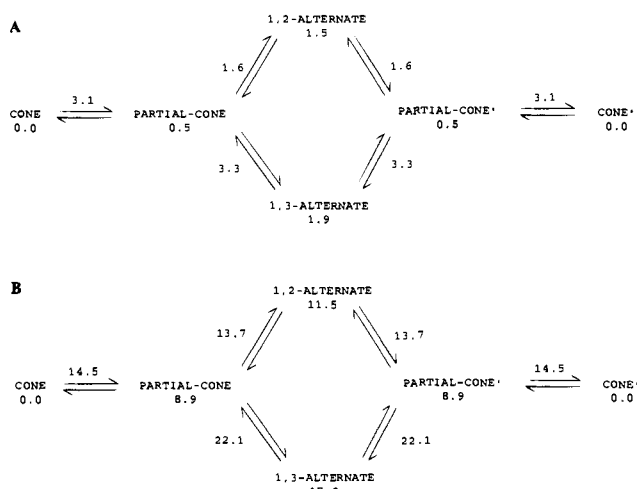


Figure 3. Connectivity chart and pathways for the Cone \rightarrow Cone' conversion: (A) cyclophane **3a**, (B) calix[4]arene **1a**. The numbers are the energies (E_{conf}) of the stable conformers or $E_{\text{conf}}^{\ddagger}$ of the transition state of the reactions (in kcal/mol, corrected for conformational degeneracy, see text and Tables 1 and 3).

mol, the energy of activation of the Cone \rightarrow Paco transition corrected for this conformational entropy is $\Delta E_{\text{conf}}^{\ddagger} = \Delta E_{\text{pot}}^{\ddagger} - kT \ln 4$. At -30°C , $\Delta E_{\text{conf}}^{\ddagger} = 3.1$ kcal/mol, which is below the upper limit of $\Delta G^{\ddagger} < 5.9$ kcal/mol deduced from ^1H NMR measurements for the Cone \rightarrow Cone' conversion.^{19d} These results agree with the experimental observations that conformational interconversions in [1₄]metacyclophanes are very fast.¹⁹ $\Delta E_{\text{conf}}^{\ddagger}$ is computed for all reactions listed in Table 3 by comparing the conformational degeneracy of the saddle points to the degeneracy of the ground state (see Discussion).

(ii) **Stepwise Interconversion in 1a.** For compound **1a**, both stepwise (involving a single phenyl ring flip at a time) and direct (involving more than one ring-flip) interconversion pathways were calculated. The stepwise Cone \rightarrow Inverted Cone (Cone') reaction was investigated by individually refining the Cone \rightarrow Paco, Paco \rightarrow 1,2Alt, and Paco \rightarrow 1,3Alt paths. The direct Cone \rightarrow 1,2Alt, Cone \rightarrow 1,3Alt, and Cone \rightarrow Cone' paths were also refined. The direct Cone \rightarrow 1,2Alt path has the same saddle points as the stepwise Cone \rightarrow Paco \rightarrow 1,2Alt pathway. Similarly, the direct Cone \rightarrow 1,3Alt path proceeds via the stepwise Cone \rightarrow Paco \rightarrow 1,3Alt pathway. The direct Cone \rightarrow Cone' path also proceeds via a stepwise pathway, so that all interconversions in **1a** can be broken down into three reaction steps, whose transition-state energies are listed in Table 3. The corresponding potential energy profiles along these reactions

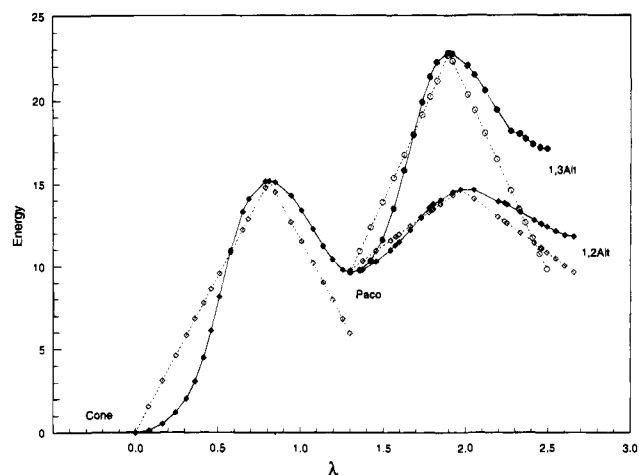


Figure 4. Energy profile (solid line, kcal/mol) and Hammond correlation H_i (dashed line, see text) for the stepwise ring-flipping isomerization reactions in compound **1a**. Shown are the Cone \rightarrow Paco, Paco \rightarrow 1,2Alt, and Paco \rightarrow 1,3Alt paths. λ is the curvilinear reaction coordinate, in Å (see Methods section).

are shown in Figure 4. Concerted paths, with two or more rings flipping simultaneously, were not found. Figure 3B shows the possible pathways for a Cone \rightarrow Cone' interconversion. The overall rate-limiting step (as defined by the highest energy barrier) of the Cone \rightarrow Cone' interconversion is the Cone \rightarrow Paco transition, with an activation barrier of $\Delta E_{\text{pot}}^{\ddagger} = 15.2$ kcal/mol. The pathway then proceeds via the 1,2Alt conformer, which has a much lower barrier than the Paco \rightarrow 1,3Alt path. Accounting for the conformational entropy of the Cone \rightarrow Paco transition (see previous section and Discussion), $\Delta E_{\text{conf}}^{\ddagger} = 14.5$ kcal/mol, in excellent agreement with the experimental ΔH^{\ddagger} value of 14.2 kcal/mol in CDCl_3 as determined by ^1H NMR for the Cone \rightarrow Cone' interconversion.^{13c} Much of the barrier comes from breaking two hydrogen bonds, which amounts to $\Delta E_{\text{elec}}^{\ddagger} = 9.1$ kcal/mol. Most of the remainder of the activation barrier comes from the deformation of some bond angles, such as the AR-CH-AR angles (from 110° to 120°) of the two methylene groups to which the rotating ring is attached, with $\Delta E_{\text{angle}}^{\ddagger} = 5.9$ kcal/mol. In the transition state, the rotating ring makes an angle of $\sim -20^{\circ}$ with the mean plane of the four methylene carbon atoms, which means that the phenol group has partly passed through the plane of the methylene carbon atoms (Figure 5). During the transition, the opposite phenol ring rotates to be more in plane with the annulus, whereas the other two phenol rings move the other way and become closer to perpendicular to the plane of the methylene groups.

Earlier reaction path calculations have been performed on **1c** by forcing internal rotations around an axis going through the two methylene groups attached to the phenolic ring.³ This torsion angle was constrained and the rest of the calix[4]arene was relaxed by energy minimization. The resulting energy barriers for the interconversions Cone \rightarrow Paco, Paco \rightarrow 1,2Alt, and Paco \rightarrow 1,3Alt were 8.1, 8.9, and 9.4 kcal/mol, respectively. The force field used, MM2P,⁹ treated the hydrogen bonds only in a qualitative way, so that lower barriers were obtained even though the optimal path was not followed. The predefined reaction coordinate did not ensure full relaxation during the interconversion and the maxima along this reduced adiabatic path were not resolved to true saddle points.

(iii) **Concerted Interconversion in 1a.** Investigation of the strength of the hydrogen bonds in calix[4]arenes with IR spectroscopy in CCl_4 has suggested that the hydrogen bonding in calix[4]arenes may be cooperative, i.e. the breaking of the first H-bond in the circular array of four H-bonds is more difficult than the breaking of additional H-bonds. This is

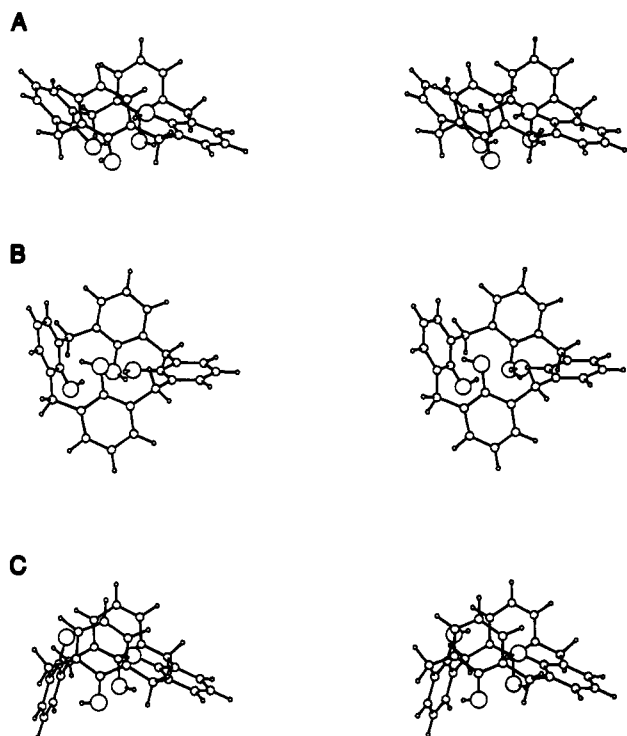


Figure 5. Saddle-point structure (stereo) of the ring-flipping isomerizations in compound **1a**: (A) Cone \rightarrow Paco, (B) Paco \rightarrow 1,2Alt, (C) Paco \rightarrow 1,3Alt. In each case, the converting ring is on the right and is rotating clockwise for the indicated reaction direction.

believed to be caused by polarization of the O—H bonds in the circular array.¹⁵ The polarization effect in **1a** was investigated here by adding a charge Δq to the hydrogens and $-\Delta q$ to the oxygens of the hydroxyl groups. For every Δq , the conformers were reoptimized and the direct Cone \rightarrow 1,2Alt and Cone \rightarrow 3,1Alt conversion pathways were refined. In each case, the stepwise pathways through the Paco intermediate become a concerted movement of the phenol rings when $\Delta q \geq 0.35$ e, as denoted by the presence of a single saddle point instead of two successive saddle points along the path. With $\Delta q = 0.35$, resulting in a partial charge of -0.89 e on O and $+0.78$ e on H, the potential energy of the unique saddle point relative to the reoptimized Cone is 37.4 kcal/mol for the Cone \rightarrow 1,2Alt path and 66.9 kcal/mol for the Cone \rightarrow 1,3Alt path. The structure of the transition state is respectively 1,2Alt-like and 1,3Alt-like and it is characterized by the preservation of the four hydrogen bonds in a partially distorted circular array, at the cost of considerable distortion of the calix[4]arene framework (Figure 6). The 1,2Alt[‡] conformer more readily accommodates the four hydrogen bonds than the 1,3Alt[‡] conformer, because two H-bonds are still present in the stable 1,2Alt conformer, whereas the stable 1,3Alt conformer has all four H-bonds broken. This explains why the concerted pathway via the 1,2Alt[‡] conformer is much more favorable than that via the 1,3Alt[‡] conformer. The value of Δq at which the pathway changes from a stepwise pathway to a concerted pathway coincides with the Δq at which the Paco conformation becomes a hybrid Paco/1,2Alt conformation (Figure 7). The concerted pathway via the 1,2Alt[‡] conformer resembles the proposed “continuous-chain” pathway.^{13b} While these results indicate that a “continuous-chain” pathway is in principle possible, it is unlikely because of the unrealistically large partial charges on the hydroxyl groups necessary to obtain it and because the potential energy of the 1,2Alt and the 1,3Alt conformers relative to the Cone conformer increases significantly with Δq , reaching 35.7 and 66.4 kcal/mol, respectively, when $\Delta q = 0.35$, i.e. only 1.7 and 0.5 kcal/mol less than the respective transition-state

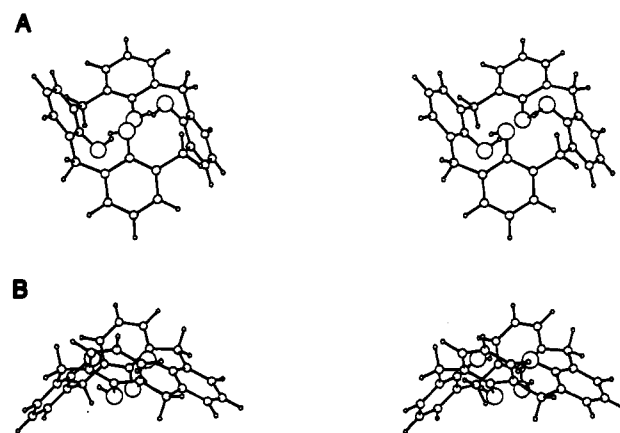


Figure 6. Saddle-point structure (stereo) of concerted ring-flipping in **1a** with hydroxyl charge separation increased by $\Delta q = 0.35$ e: (A) Paco \rightarrow 1,2Alt, (B) Paco \rightarrow 1,3Alt.

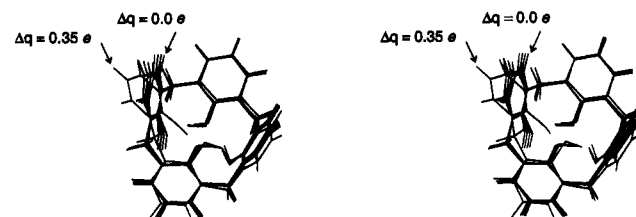


Figure 7. Optimized structures (stereo) of the **1a** Paco conformer obtained with increments in the hydroxyl charge separations Δq of 0.0, 0.1, 0.2, 0.3 and 0.35 e.

Table 4. Potential Energy (kcal/mol) of the Transition State in Isomerization Reactions of **2b**^a

reaction	$E_{\text{coval}}^{\ddagger}$	$E_{\text{vdW}}^{\ddagger}$	$E_{\text{elec}}^{\ddagger}$	$E_{\text{pot}}^{\ddagger}$	$\Delta E_{\text{pot}}^{\ddagger b}$
C_{2v} Cone \rightarrow C_{2v} Cone ^c	-0.2	0.7	2.6	3.1	
methoxy rotations					
0000~AAAA \rightarrow 0000~AABA	-3.4	4.3	8.8	9.7	5.9
0001~AAAA \rightarrow 0001~AABA	-1.8	2.0	7.8	8.0	8.0
0011~ABAB \rightarrow 0011~AAB	2.4	4.0	1.5	7.9	7.2
0101~AAAA \rightarrow 0101~AABA	-1.4	1.0	8.4	8.0	7.5
ring-flips					
0001~AABA \rightarrow 0000~AABB	12.7	9.0	-2.1	19.6	
0001~AABA \rightarrow 0011~AAAA	9.6	8.7	1.9	20.2	
0001~BBAA \rightarrow 0101~BAAA	10.7	9.1	-1.6	18.2	

^a The reactions listed here are the ones which have the lowest saddle-point energy for each given type of reaction (such as a methoxy rotation in a Cone, in a Paco, etc.). Energies are relative to the Paco ground state 0001~AABA. See also caption of Tables 1 and 2. ^b $\Delta E_{\text{pot}}^{\ddagger}$ is the energy barrier relative to the ground state of the respective characteristic conformer (i.e. Cone, Paco, etc.). ^c Energies are relative to the 0000~AAAA Cone.

energies. Most importantly, the corresponding activation barriers are irreconcilable with the kinetic data from NMR experiments (see previous section). Therefore, our calculations indicate that a concerted mechanism is unrealistic, i.e. the conversion from Cone conformer to inverted Cone conformer in **1** proceeds via a stepwise mechanism with the Paco and 1,2Alt conformers as intermediates (see Figure 3B).

(iv) **Interconversions in Calix[4]arene 2b.** For the tetramethyl ether **2b** the situation is more complicated because of the many minima that are introduced by the two possible orientations for each methoxy group (see Table 2). The orientation of the methoxy groups affects the energy barriers of the anisole ring rotations, which are large compared to the barriers of the methoxy rotations themselves. The transition-state potential energies of some methoxy rotations are listed in Table 4 and can be seen to be in the 8–10 kcal/mol range, whereas the lowest ring rotation transition states are in the 20–24 kcal/mol range. Taken relative to the ground states of each

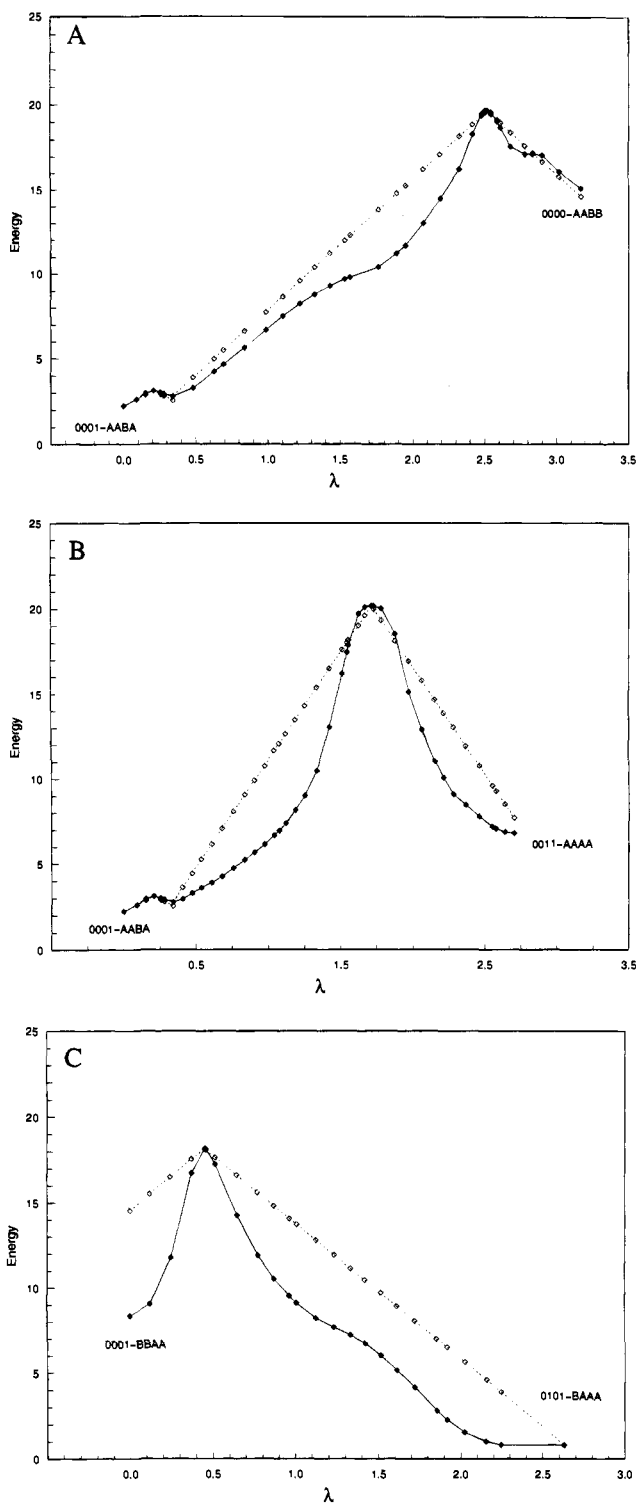


Figure 8. Energy profiles (kcal/mol) for the (A) Paco \rightarrow Cone, (B) Paco \rightarrow 1,2Alt, (C) Paco \rightarrow 1,3Alt ring-flip conversions of **2b**. See the caption of Table 2 for the nomenclature of the conformations.

of the four characteristic conformers of **2b**, the activation barriers to methoxy rotation are only 6–8 kcal/mol (Table 4). For example, the $0000\sim AAAA \rightarrow 0000\sim AABA$ reaction has a barrier of $\Delta E_{\text{pot}}^{\ddagger} = 5.9$ kcal/mol relative to the Cone ground state. A search for the preferred ring interconversion pathway cannot be limited to the conformational transitions between the reactant and product conformers with the most stable methoxy orientation, because paths for ring conversion with lower overall transition-state energy might connect characteristic conformers whose methoxy groups are not in the ground-state orientation. The conversion paths from the Paco conformer to the Cone, 1,2Alt, and 1,3Alt conformations were determined for all

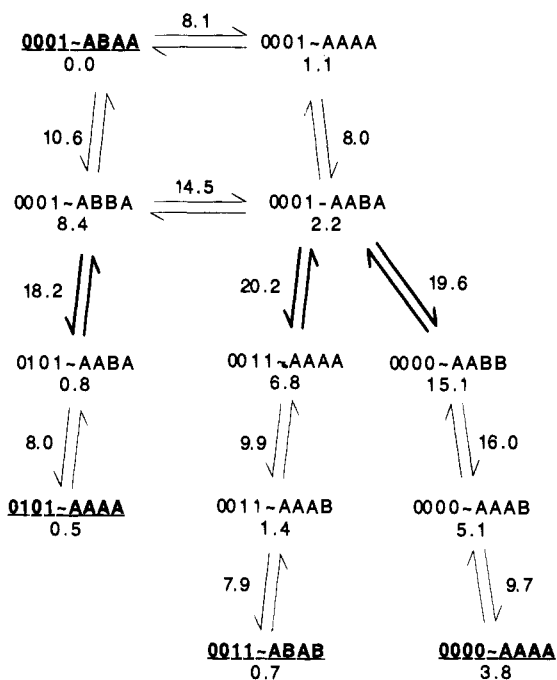


Figure 9. Connectivity chart for calix[4]arene **2b**. Shown are the lowest energy pathways connecting the ground states of the four characteristic conformers, i.e. $0001\sim ABAA$, $0101\sim AAAA$, $0011\sim ABAB$, and $0000\sim AAAA$ (see footnote of Table 2 for an explanation of the conformation names). Thick arrows: flipping of the phenyl ring. Thin arrows: methoxy rotations. The numbers are the energies E_{pot} (in kcal/mol) of the stable conformers or $E_{\text{pot}}^{\ddagger}$ of the transition state of the reactions (see Tables 2 and 4). Notice that for all transitions from one ground state to another, two or more methoxy rotations are necessary.

combinations of reactant and product methoxy orientations, for a total of 228 reactions.

The Paco \rightarrow Cone conversion with the lowest saddle point potential energy of 19.6 kcal/mol is found with $0001\sim AABA$ as the Paco reactant (Table 4), which is 2.2 kcal/mol higher than the $0001\sim ABAA$ Paco ground state (Table 2). The Paco \rightarrow Cone conversion directly from the Paco ground state yields a saddle point whose potential energy is slightly higher at 19.8 kcal/mol. The transition from the Paco ground state to $0001\sim AABA$ has a barrier of only 8.1 kcal/mol and therefore is not the rate-limiting step of the Paco \rightarrow Cone ring-flip. The situation is similar for the Paco \rightarrow 1,2Alt conversion, where the lowest transition state is also achieved when $0001\sim AABA$ is the Paco reactant, and for the Paco \rightarrow 1,3Alt transition, which proceeds from the $0001\sim BBAA$ Paco state. The smallest activation barriers relative to the Paco ground state are then 19.6, 20.2, and 18.2 kcal/mol respectively for the Paco \rightarrow Cone, Paco \rightarrow 1,2Alt and Paco \rightarrow 1,3Alt conversions. The corresponding potential energy profiles are shown in Figure 8, parts A, B, and C. The pathways connecting the four ground states of the characteristic conformers via methoxy rotation and anisole ring conversion are shown in Figure 9. In all cases, the activation energy for ring conversion is dominated by an increase of about 9 kcal/mol in van der Waals energy and an increase in bond stretch and bond angle energy of 3–6 kcal/mol. The electrostatic contribution to the barriers is smaller than in calix[4]arene **1a** and comparable to that found in compound **3a** (See Table 3), due to the lack of strong H-bonds. The conformations of the saddle points are shown in Figure 10.

The C_{4v} symmetric Cone of **2b** has been proposed² to be the saddle point of the interchange of two equivalent C_{2v} symmetric Cone conformations. In the C_{2v} form, the planes of two facing anisole rings are almost parallel to each other (“pinched”) and

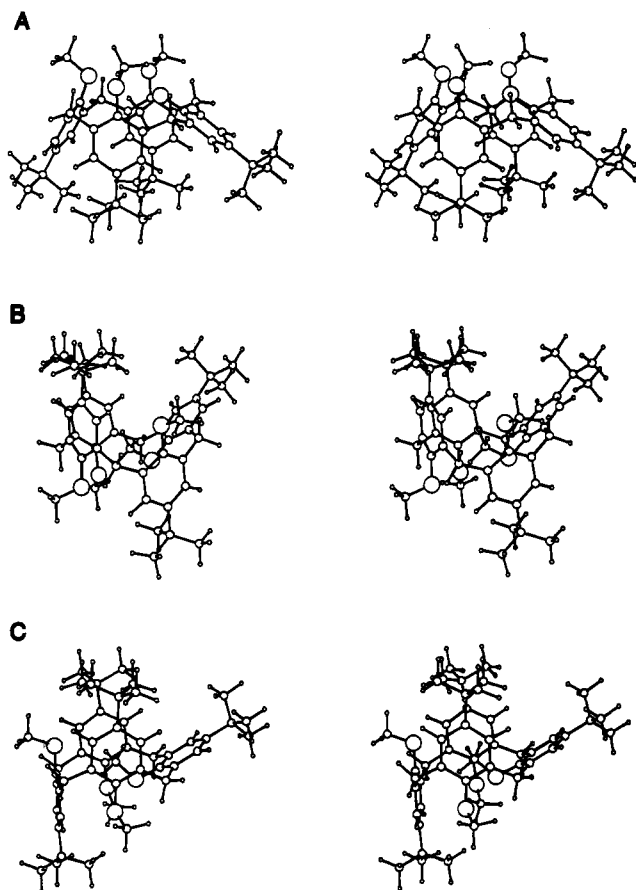


Figure 10. Saddle-point structures (stereo) of the ring-flipping isomerizations in compound **2b**: (A) $0001 \sim AABA \rightarrow 0000 \sim AABB$, (B) $0001 \sim AABA \rightarrow 0011 \sim AAAA$, (C) $0001 \sim BBAA \rightarrow 0101 \sim BAAA$. In each case, the converting ring is on the right and is rotating clockwise for the indicated reaction direction. See footnote of Table 2 for an explanation of the conformation names.

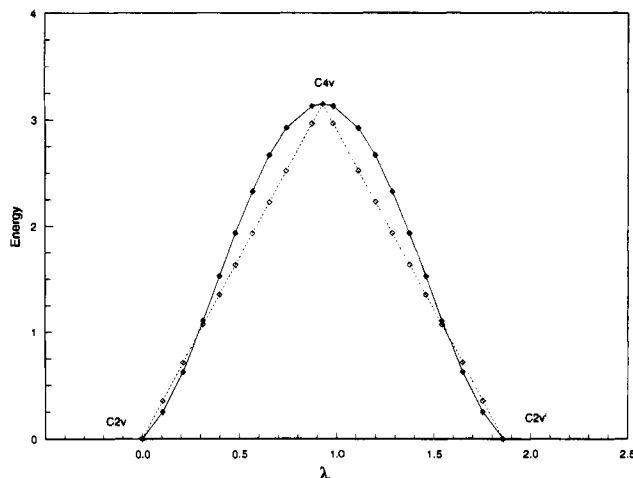


Figure 11. Energy profile (solid line, kcal/mol) and Hammond correlation (dashed line) for the conversion from one C_{2v} Cone to the other in **2b**.

orthogonal to the annulus while the other two anisole rings are more coplanar with the annulus, unlike the C_{4v} Cone which has the four rings at the same angle relative to the plane of the annulus. We have calculated the transition from one $0000 \sim AAAA$ C_{2v} Cone to the other (Figure 11). The saddle point is only 3.1 kcal/mol higher in potential energy than the C_{2v} Cone and is indeed a C_{4v} Cone. A comparable result was obtained by constrained energy minimization using the AMBER 3.0 force field.² $C_{2v} \rightarrow C_{2v}'$ transitions have been observed during molecular dynamics simulations³¹ of lower rim substituted

derivatives of **2**. The type of lower ring substituent affects the propensity for the C_{2v} form.²

Discussion

The distribution^{7,4a} of the conformations of **2b** as determined with ^1H NMR in CDCl_3 at -30°C is 85% Paco, 8% 1,2Alt, 4% Cone, and 3% 1,3Alt. The accuracy in these particular NMR spectra is expected to be around 2% (absolute). The Boltzmann weighted probability of finding compound **2b** in state x , corrected for the conformational degeneracy and neglecting vibrational effects on relative populations (vibrational and rotational contributions to the free energy will be presented elsewhere), is given by³²

$$p(x) = \frac{\sum_{i \in Cx} n_i e^{-E_i/kT}}{\Omega}$$

where n_i is the degeneracy of conformer i and E_i is the potential energy (both given in Table 2). Ω is the partition function

$$\Omega = \sum_{\text{all } j} n_j e^{-E_j/kT}$$

For example, there are two possible AAAA Cones for compound **2b**, $0000 \sim AAAA$ and $1111 \sim AAAA$, so the degeneracy of that conformer is $n = 2$. With the data in Table 2, $p(\text{Paco}) = 63.3\%$, $p(1,2\text{Alt}) = 18.4\%$, $p(1,3\text{Alt}) = 18.3\%$, and $p(\text{Cone}) = 0.006\%$ at -30°C . The Paco state is correctly predicted as the most probable conformation, but its calculated probability is somewhat lower than the experimental one. Also, the order of the abundance of the Cone and 1,3Alt forms is inverted.

If the relative energy differences due to methoxy rotation are assumed to be correct within each characteristic conformer of **2b** and a constant correction term ΔE_x is added to the potential energy (as given in Table 2) of every conformer in the characteristic state x , then the exact experimental distribution is obtained for $\Delta E_{\text{Paco}} \equiv 0.0$, $\Delta E_{1,2\text{Alt}} = +0.54$ kcal/mol, $\Delta E_{1,3\text{Alt}} = +1.0$ kcal/mol, and $\Delta E_{\text{Cone}} = -3.0$ kcal/mol. If only the lowest conformer of each type is considered, the result is $\Delta E_{\text{Paco}} \equiv 0.0$, $\Delta E_{1,2\text{Alt}} = +0.44$ kcal/mol, $\Delta E_{1,3\text{Alt}} = +0.43$ kcal/mol, and $\Delta E_{\text{Cone}} = -3.0$ kcal/mol. With the MM3 force field, the following relative stabilities have been found:⁴ Paco > 1,3Alt \approx Cone > 1,2Alt, i.e. the ranking of the Cone was consistent with experimental data, but the 1,3Alt and 1,2Alt were inverted. A study² with the AMBER 3.0 force field resulted in 1,3Alt > Paco > Cone > 1,2Alt. Quantitatively correct values are difficult to achieve, due to the complex balance of forces, particularly between covalent and electrostatic terms (see Table 2).

The Paco conformation has a high field position ($\delta = 1.99$ ppm) for one of its three methoxy signals in the ^1H NMR spectrum of **2b** in CDCl_3 ,⁷ indicating that one strongly shielded methoxy group is pointing inwards. This agrees with two of the three most stable Paco forms found here, $0001 \sim ABAA$ and $0001 \sim AAAB$ (Table 2), which both have one methoxy pointing inward. The Cone has one single low field methoxy signal ($\delta = 3.83$ ppm), indicating that the four unshielded methoxy groups are pointing outwards. This is consistent with the most stable Cone conformer, which has all methoxy groups pointing out ($0000 \sim AAAA$ in Table 2). In the 1,2Alt and 1,3Alt conformers, the four methoxy groups show one single intermediate field

(31) Guillaud, P.; Vamek, A.; Wipff, G. *J. Am. Chem. Soc.* **1993**, *115*, 8298–8312.

(32) McQuarrie, D. A. *Statistical Mechanics*; Harper & Row: New York, 1976.

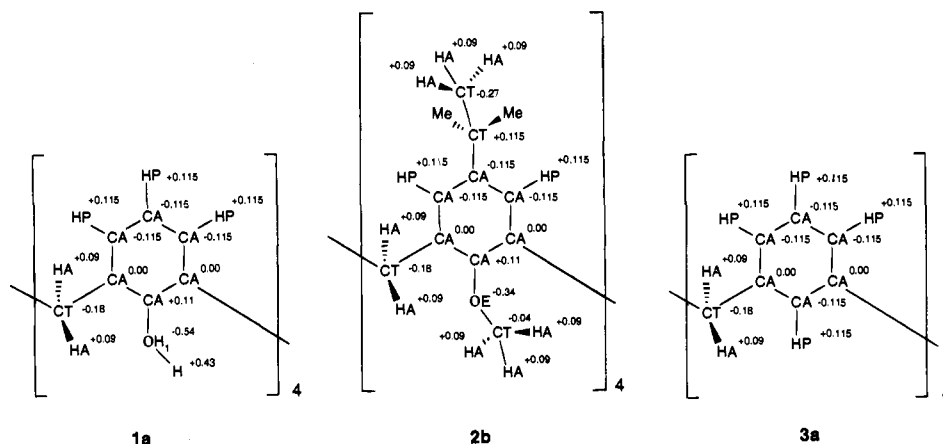


Figure 12. Atom types and partial charges of 1a, 2b, and 3a.

Table 5. van der Waals Parameters

atom type	E_{\min} (kcal mol ⁻¹)	$R_{\min}/2$ (Å)	atom type	E_{\min} (kcal mol ⁻¹)	$R_{\min}/2$ (Å)
CA	-0.0700	1.9924	HP	-0.0300	1.3582
CT	-0.1562	1.8000	H	-0.0460	0.2245
HA	-0.0078	1.468	OE	-0.1200	1.7700
OH1	-0.1521	1.7700			

signal ($\delta = 2.99$ ppm for the 1,2Alt conformer and $\delta = 2.87$ ppm for the 1,3Alt conformer). This means that either the four methoxy groups are pointing inward and have intermediate shielding or there is fast exchange between the strongly shielded inward and the unshielded outward orientations. From the calculations, having four methoxy groups pointing inward is very unfavorable. The 1,3Alt is only able to accommodate all four methoxy groups pointing inwards at a cost of 12.9 kcal/mol relative to the all-out 1,3Alt conformer. The all-inward conformation of 1,2Alt is unstable. This suggests that in both the 1,2Alt and the 1,3Alt conformers there is a fast exchange between conformations with methoxy groups pointing inward and outward. For example, the most populated 1,2Alt conformer (ABAB) has two methoxy groups in and two out. If the methoxy groups are rapidly interchanging (ABAB \leftrightarrow BABA), a single intermediate field signal is expected. This is consistent with the calculations, which show that the methoxy rotations in the 1,2Alt and 1,3Alt conformers have low transition barriers relative to their respective ground states (ΔE^*_{pot} in Table 4). The rate of interconversion between two species at a temperature where their signals have just coalesced in the spectrum (the coalescence temperature) can be estimated from the separation of the two signals (in Hz) at a low temperature where the two species are not exchanging. An upper limit to the barrier for methoxy rotation can be estimated for the 1,2Alt and 1,3Alt conformers, whose inward and outward methoxy signals have coalesced. If one takes 1.84 ppm as an upper bound to the separation between the inward and outward methoxy signals (from the observed values of the methoxy signals, 1.99 ppm inward in Paco and 3.83 ppm outward in Cone), this corresponds to 1104 Hz at 600 MHz. Assuming Arrhenius kinetics, equal population of the two states, and -30 °C as the coalescence temperature, the energy barrier to methoxy rotation is $\Delta E^* \leq 10.7$ kcal/mol. Our calculated barriers for methoxy rotation (ΔE^*_{pot} in Table 4) are in agreement with this limiting value.

The ¹H NMR data for the Cone conformation of 2b are consistent with either a C_{4v} symmetric Cone or the average structure resulting from the rapid interconversion between the two possible C_{2v} Cone conformers, in which the C_{4v} Cone is the transition state.² The optimized geometry of the 2b Cone has C_{2v} symmetry ("pinched Cone", see Results section). We found the C_{4v} Cone to be the saddle point in the interconversion

Table 6. Bonded Parameters

bond	K_b (kcal mol ⁻¹ Å ⁻²)	r_0 (Å)
CA-OE	296.70	1.450
CT-OE	296.70	1.450
CA-CA	305.00	1.375
CT-CA	230.00	1.490
OH1-CA	334.30	1.411
OH1-H	545.00	0.960
HP-CA	340.00	1.080
CT-CT	229.63	1.531
HA-CT	317.13	1.111

angle/Urey-Bradley	K_θ (kcal mol ⁻¹ Rad ⁻²)	θ_0 (deg)	F (kcal mol ⁻¹)	l_0 (Å)
CA-CT-CA	52.000	109.47		
CA-CA-OE	45.200	120.00		
CA-OE-CT	110.00	109.7		
OE-CT-HA	45.200	107.24		
H-OH1-CA	65.000	108.00		
OH1-CA-CA	45.200	120.00		
CA-CA-CA	40.000	120.00	35.00	2.4162
CT-CA-CA	45.800	122.30		
CT-CT-CA	51.800	107.50		
HA-CT-CT	33.430	110.10	22.53	2.1790
HA-CT-CA	49.300	107.50		
CT-CT-CT	58.350	113.50	11.16	2.5610
HP-CA-CA	30.000	120.00	22.00	2.1525
HA-CT-HA	36.000	108.40	5.20	1.8020

dihedral angle	K_ϕ (kcal mol ⁻¹)	n	ϕ (deg)
OE-CA-CA-CT	3.10	2	180.00
CA-CA-OE-CT	1.40	2	180.00
OE-CA-CA-CA	3.10	2	180.00
OE-CA-CA-CT	3.10	2	180.00
OE-CA-CA-HP	3.10	2	180.00
HP-CA-CA-HP	2.40	2	180.00
OH1-CA-CA-CT	3.10	2	180.00
H-OH1-CA-CA	0.98	2	180.00
OH1-CA-CA-CA	3.10	2	180.00
HA-CT-OE-CA	0.10	3	0.00
CA-CA-CA-CA	3.10	2	180.00
CT-CA-CA-CA	3.10	2	180.00
HP-CA-CA-CA	4.20	2	180.00
HP-CA-CA-CT	4.20	2	180.00
CT-CT-CA-CA	0.23	2	180.00
HA-CT-CT-CA	0.05	3	0.00
X-CT-CT-X	0.16	3	0.00
X-CT-CA-X	0.00	2	180.00

from one C_{2v} Cone to the other, with an activation barrier of 3.1 kcal/mol, which suggests that fast interconversion is occurring.

The 2D EXSY NMR spectra of a calixcrown derivative of 2a, which has two facing rings bridged at the upper rim so that the formation of the 1,2Alt conformer is prevented, have shown that Paco can convert to Cone and to 1,3Alt conformers.¹⁶ The

conversion to the 1,3Alt conformer is faster than conversion to the Cone conformer. This is in accord with the respective activation barriers of 18.2 and 19.6 kcal/mol calculated here (see Table 4). Measurements on **2b** with ^1H and 2D EXSY NMR indicate that the conversions from Paco to Cone or to 1,3Alt are faster than the conversion from Paco to the 1,2Alt conformer.⁷ This is also consistent with the higher activation barrier of the Paco \rightarrow 1,2Alt path (20.2 kcal/mol in Table 4).

The pertinence of the Hammond postulate to interconversion reactions in calix[4]arenes was tested by correlating the root-mean-square (rms) displacement of the atomic positions with the energy of the system (see Methods section). In most cases, the reaction energy profiles (see Figures 2, 4, 8, and 11) show an excellent correlation with the change in rms of the atomic positions along the path, indicating that the conformational changes in calix[4]arenes obey the Hammond postulate.

Although no solvent effects were included in the calculations, close agreement has been found between the calculated and experimental ΔH^\ddagger for the Cone \rightarrow inverted-Cone conversion of **1a** in CDCl_3 . This is not surprising, since the ΔG^\ddagger as determined by ^1H NMR is nearly solvent independent.^{13b} In contrast, the conformational distribution of **2b** found by ^1H NMR is influenced by the solvent,¹⁵ mostly changes in the abundance of the Cone form at the cost of the other forms: 5% Cone in CDCl_3 , 14% Cone in CS_2 and CCl_4 , 18% Cone in toluene. Explanations for this behavior have been sought either in terms of the polarity of the solvent³³ or by the inclusion of a solvent molecule in the cavity of the Cone.^{15,31} Solvent polarity cannot explain all the solvent effect data; e.g. the Cone conformer of **2b** is more abundant in CCl_4 than in CDCl_3 , although the latter is the more polar solvent and the Cone is the conformation with the largest dipole moment, which would be expected to be more abundant in a more polar solvent.¹⁵ More likely, enlargement of the cavity in the *tert*-butyl-substituted calix[4]arenes allows for complex formation with the solvent.^{14,17}

Conclusions

The energies and conformational transitions of calix[4]arenes **1a** and **2b** and [1₄]metacyclophane **3a** have been studied using the CHARMM molecular mechanics potential with the new parameter set 22. Although these parameters were developed for amino acids, they could be used without modification. The relative stabilities for the four conformations of the three compounds are in good agreement with experimental NMR data. The same is true for the activation barriers of the ring interconversions between the characteristic conformers of **1a**, **2b**, and **3a** and of the methoxy rotations in **2b**. The present study provides detailed information concerning the calculated pathways connecting the various conformers. This was made possible by the CPR algorithm, which has been implemented in the CHARMM program. In the absence of an initial guess for transition intermediates, the method starts with a linear interpolation pathway from the reactant to the product conformation, which is then refined. In nearly every case, this was sufficient to yield the pathway with the lowest activation barrier for the Cone \rightarrow Cone' conversions. Only in **1a** did a stepwise refinement of Cone \rightarrow Paco followed by Paco \rightarrow 1,2Alt find a lower saddle point than the direct Cone \rightarrow Cone' calculation, which proceeded via the 1,3Alt intermediate.

The pathways for [1₄]metacyclophane **3a** Cone \rightarrow Cone' interconversion show no marked preference for the 1,2Alt or 1,3Alt intermediate. The structure of the **1a** Cone form is close

to the Cone form of the **3a** [1₄]metacyclophane, indicating that the circular array of H-bonds in **1a** puts little additional strain on the calix[4]arene frame. The most likely Cone \rightarrow Cone' conversion of **1a** is along a stepwise Cone \rightarrow Paco \rightarrow 1,2Alt \rightarrow Paco' \rightarrow Cone' pathway. The hypothesis of a concerted mechanism, in which the four phenol rings of **1a** would corotate to conserve the four H-bonds, is not consistent with the present calculations, as demonstrated by the excessive hydroxyl O-H bond polarization necessary to achieve such a mechanism. The relative stability of the **2b** characteristic conformers is affected by the conformational degeneracy of the energy states due to the symmetry of the molecule. Even though the 1,2Alt form 0011~ABAB is ranked higher in terms of potential energy than the 1,3Alt form 0101~AAAA, consideration of the conformational degeneracy reveals that the former is more stable than the latter, in accordance with experiment. Similarly, the stability ranking of the 1,3Alt forms 0101~AAAA and 0101~AABA, differing by their methoxy orientations, is inverted after inclusion of the conformational degeneracy of these structures.

Interconversions between the characteristic conformers of **2b** occur with the Paco form as the key intermediate. The anisole ring interconversions with the lowest absolute transition-state energies are not between the ground states of the respective characteristic conformers but between conformations that are related to their ground states via one (in the case of 1,3Alt), two (in the case of Cone and 1,2Alt), or up to three (in the case of Paco) rotations of the methoxy groups. Rotations of the methoxy moieties have energy barriers well below the energy barriers for anisole ring rotation, explaining why the methoxy hydrogens give a single peak in ^1H NMR. The NMR data in favor of a C_{4v} symmetric Cone, i.e., the aromatic protons appear as one singlet and the protons on the methylene bridges appear as an ABq system, can be explained by the low barrier between the two stable C_{2v} forms, which allows fast exchange on the NMR time scale.

The present analysis demonstrates the power of molecular mechanics combined with an efficient and general technique for finding reaction paths to explore in detail the connectivity on potential energy surfaces of complex molecules with multiple conformers.

Note Added in Proof: M. Hosseini pointed out the paper by K. B. Lipkowitz and G. Pearl [*J. Org. Chem.* **1993**, 58, 6729–6736] in which molecular mechanics calculations with different programs for a number of calix[4]arenes were reported. Species **2b** is the only one that was calculated by Lipkowitz and Pearl, as well as in the present paper. In contrast to their results, we find good agreement with experiment. G. Wipff and M. Lauterbach (private communication) have obtained energy differences similar to those reported in the present paper; they have also studied the effect of solvent on the energy differences.

Acknowledgment. The work reported here was supported in part by a grant from the National Science Foundation and a gift from Molecular Simulations Inc. to Harvard University.

Appendix

New molecular mechanics parameters were used for the calix[4]arenes in this study. Figure 12 shows the atom types and their partial charges. The nonbonded van der Waals parameters are given in Table 5 and the bonded parameters in Table 6.

(33) Iwamoto, K.; Ikeda, A.; Araki, K.; Harada, T.; Shinkai, S. *Tetrahedron* **1993**, 49, 9937–9946.